MECHANICAL PROPERTIES, PHYSICS OF STRENGTH, AND PLASTICITY

Folding in FCC Metal Single Crystals under Compression

D. V. Lychagin[a], * and E. A. Alfyorova[b], **

a National Research Tomsk State University, pr. Lenina 36, Tomsk, 634050 Russia
b National Research Tomsk Polytechnic University, pr. Lenina 30, Tomsk, 634050 Russia
* e-mail: dvl-tomsk@mail.ru
** katerina525@mail.ru
Received July 7, 2014; in final form, September 23, 2014

Abstract—Results of the analysis of folding during compression deformation of metals with fcc lattice are presented. Single crystals with orientations at angles of the standard stereographic triangle and different crystallographic orientations of lateral faces have been studied. It has been found that the major factor affecting the folding intensity is the slip plane shear with respect to lateral faces. Such a shear results in face bending and the formation of fold systems in maximum curvature regions. It has been shown that, among all considered orientations, the maximum susceptibility to the formation of different folds is inherent in single crystals with $[\bar{1}11]$ compression axis orientation. For this orientation, the development of shear and rotational components during folding is traced by interference microscopy and electron backscatter diffraction methods. It has been found that an excess dislocation density is accumulated when shear is activated in the folding region, which results in an increase in fold misorientation. The activation of this process in fcc metals is promoted by an increase in the homologous deformation temperature and stacking fault energy.

1. INTRODUCTION

The folding and corrugating phenomenon attracts attention of specialists in different science and engineering fields. An analysis of the corrugating process is directed to the prediction of obtaining this or that material structure after pressure treatment and, hence, metal service properties. The determination of the causes of folding makes it possible to control this process, which, in turn, will improve the quality of produced articles.

The large number of papers by Gubernatorov et al. are devoted to the study of the corrugation process [1–4]. They found that a specific inhomogeneity type appears in the creep nucleus during plastic deformation, which is caused by material layer planarity distortion; in turn, this results in corrugated structure formation [4]. As a possible cause of the corrugation formation, the hypotheses of stability loss by material layers which are subjected to constrained deformation and the appearance of sign-alternating stresses at the mesolevel is proposed. Hence, such a structure can be formed even without basic stress concentrators. In [2], based on the corrugation concept, a geometrical model of material structure and texture formation was developed. In [3], it was experimentally proved that the deformation structure shaped as a corrugation is formed in both initially structurally inhomogeneous and structurally homogenous materials (single crystals). Taking this into account, it is concluded that

exactly material corrugation forms its textural and structural state.

The works in which the development of the deformation relief under compression of single-crystal samples is studied [5, 6] suggest that folds represent an integral part of the relief. Micro-, meso-, and macroscopic-size folds are observed. The studies on single crystals are modeling; however, the study of the physical nature of folding in the single crystals of pure metals seems to be reasonable. This is caused by certain geometry of dislocation glide and no effect of grain boundaries. The study of folding processes promotes profound understanding of relaxation and accommodation mechanisms of surface stresses when using different surface treatment and deformation methods and can be useful in developing materials processing.

Based on the above, it seems to be important to study folding on side single-crystal surfaces and to analyze the folding conditions.

2. MATERIAL AND EXPERIMENTAL TECHNIQUE

Single crystals with different stacking fault energies (SFE), namely, aluminum (170–300 mJ/m²), nickel (120–150 mJ/m²), and copper (40–60 mJ/m²) with compression axis orientations at angles of the standard stereographic triangle and different sets of lateral faces, were studied. The technique for preparing and studying samples was described in [6, 7]. The sample

structure was studied in intervals of true (logarithmic) degrees of deformation from 3 to 60%. The compression deformation was performed using an Instron ElektroPuls E10000 testing machine with a rate of $1.4 \times 10^{-3} s^{-1}$ at room temperature. The deformation relief was studied using a Leica DM 2500P optical microscope and a Tescan Vega II LMU scanning electron microscope with an EBSD attachment for analyzing misorientations. The deformation relief parameters were determined using a NewView 7200 microinterferometer.

3. EXPERIMENTAL RESULTS

The formation of the folded structure on the single-crystal surfaces can be observed at different orientations of sample compression axes. In each case, it will have specific features. When considering folds, attention should be paid to the degree of deformation and folding region. First of all, folds are formed during plastic deformation in the near-end zone in the beading region.

An analysis of the studied fcc single crystals of pure metals showed that the susceptibility to folding depends on the crystallographic orientation of the compression axis and lateral faces. Single crystals with the [001] compression axis with (100) and (110) lateral faces and [110] single crystals with (001) and ($\bar{1}$10) lateral faces deformed at room temperature are not susceptible to folding at moderate degrees of deformation. Single crystals with [$\bar{1}$11] compression axis are most susceptible to the formation of folded structures. At high degrees of deformation, the single-crystal shape significantly changes. This process is accompanied by significant folding.

A crystallographic analysis of the arrangement of octahedral planes in the single-crystal bulk showed that all studied single-crystal orientations can be divided into three groups. Orientations in which the slip planes are inscribed symmetrically with respect to the compression axis and lateral faces of the sample, and orientations in which slip planes are inscribed asymmetrically. The latter case promotes the bending and folding of the faces not only in the near-end zone, but also in the central sample region. Asymmetric orientation of slip planes in the single-crystal bulk increases the probability of face bending of the symmetrically oriented single crystal, hence, the probability of folding, which is implemented, e.g., in [110] single crystals with the other set of (112) and (111) lateral faces.

As noted above, the [$\bar{1}$11] orientation is least stable to the bending and folding of the faces at moderate degrees of deformation. However, as previous studies [6] showed, the least stability is observed for the samples shaped as tetragonal prisms ((110) and (1$\bar{1}$2) lat-

eral faces). The samples shaped as trigonal prisms ((110) and (112) lateral faces) have a higher stability to folding. We note that an additional distinctive feature of this orientation is the formation of macrodeformation band systems and the presence of "complicated" shear regions (based on the consideration of the crystallographic diagram of the arrangement of close-packed planes in the sample bulk). Both factors affect the folding place in samples.

When comparing [$\bar{1}$11] single crystals of different metals, we also observed the difference in folding. In what follows, we present the results obtained for samples shaped as tetragonal prisms. Most folds in copper single crystals are observed on (1$\bar{1}$2) faces, where they occupy to 80−85% of the area (13% degree of deformation); on (110) faces, the area fraction occupied by folds is 30−35%. In nickel single crystals, at a 10% degree of deformation, these values are 32% and 3%, respectively. The different areas occupied by folds on mutually perpendicular faces are also explained by the arrangement of octahedral planes in the sample volume and their different contributions to the face shape change. The shear development is accompanied by the bending of the sample faces, first of all, the (1$\bar{1}$2) face. The result is that the earliest folding is observed on this face.

Among all studied metals, aluminum has the highest stacking fault energy and the homologous deformation temperature. A characteristic feature of this material is the development of small folds near the end and normally to effective macroband systems. An individual system of folds is formed in these regions. The feature of folding regions near single-crystal ends in the case of [$\bar{1}$11] single crystals and the entire relief pattern on sample faces are determined by the existence of the center of symmetry (inversion center) during deformation.

Several folding types are observed in the near-end region in aluminum: macrofolds (beading region) and mesofolds occupying a significant area on one crystal face and a narrow area on the other crystal face. Along with folding near test machine punches, folding perpendicular to macrobands can be observed. In this case, the effect of more intense folding perpendicular to less developed macroband systems (folds F1 in Fig. 1a) is observed. This process is most pronounced in aluminum single crystals. Folds are formed normally to macroband boundaries and form a bamboo structure which becomes finer as the degree of deformation increases (Fig. 1b).

Deformation in the macroband system provides shape change only in the region occupied by this system; therefore, additional mechanisms at meso- and macrolevels are required to deform other crystal regions. As a result, we can observe the formation of
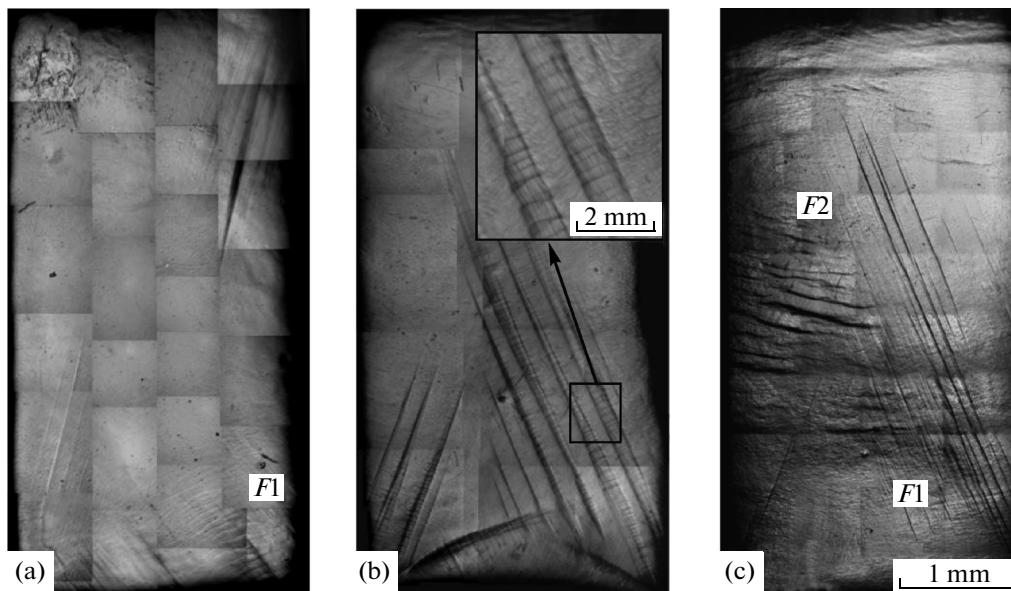
Fig. 1. (a) Deformation relief on the (110 lateral face of the [$\bar{1}$11] aluminum single crystals after a 5% degree of deformation, (b) the structure of folds on the (1$\bar{1}$2) lateral face of the [$\bar{1}$11] aluminum single crystals after a 9% degree of deformation, and (c) the strain relief on the (1$\bar{1}$2) lateral face of the [$\bar{1}$11] nickel single crystals after a 10% degree of deformation.

fold systems $F2$ in regions adjacent to regions occupied by macroband systems (Fig. 1c).

At the same time, folding in nickel and copper differs from folding in aluminum in both the degree of folding development at equivalent degrees of deformation and folding localization regions. The homologous deformation temperature has the most noticeable effect on the beading region size in the near-end zone. Meanwhile, as is known, the formation of misorientation subboundaries is enhanced by dislocation cross slip whose probability increases with the SFE. At the same time, the face area fraction occupied by folds depends to a greater extent on the crystallographic factor (the degree of accuracy of the compression axis and lateral face orientation). This complicates a more detailed analysis of the effect of the homologous deformation temperature and SFE on folding.

The study of the shear accumulation in folds, performed using interference microscopy (Fig. 2), and an analysis of the shear crystallography in [$\bar{1}$11] single crystals showed that folds at a 10% degree of deformation are formed by shear along octahedral planes. In Fig. 2c, we can show individual shear steps; the shear in folds is 80−350 nm. Hence, their formation requires 300−1500 dislocations (since the Burgers vector of nickel is $b = 0.249$ nm).

Within the present work, the folded structure was studied using the electron backscatter diffraction (EBSD) analysis. The maps obtained using the EBSD analysis (Fig. 3) illustrate the distribution of local regions with different orientations do allow us to determine misorientations in them. Figure 3 shows the misorientation pattern in the region of the formation of macroband systems and folds perpendicular to them (the region under consideration is in the uniaxial compression region). As the degrees of deformation increases, an excess dislocation density within the crystal is accumulated, which promotes the development of the misorientation [8]. In this region, the misorientation angles are ~2°.

In this case, when considering changes in misorientation angles along the secant indicated by the arrow in Fig. 3a, we can see the periodic angle variation. The maximum misorientation angles are observed with a step of ~5 μm. A similar pattern is observed when considering the folded structure at the boundary of regions with different stressed state schemes with the only difference that misorientation angles reach 8° at fold boundaries.

A specific folded structure is formed in the macrobending region on the (112) face, which is formed due to the face bending resulting from the work of the macroband systems observed on the (110) face. An analysis showed that folds of this type at a 16% degree of deformation represent an alternation of regions with initial [$\bar{1}$11] orientation with respect to the compression axis and regions with newly formed [110] orientation. In this case, the transition to the [110] orientation occurs gradually via intermediate orientations lying on the [111]−[110] stereographic triangle side. The width of not reoriented regions and regions with new orientation is ~5−9 μm and 2−3 μm. In this case,
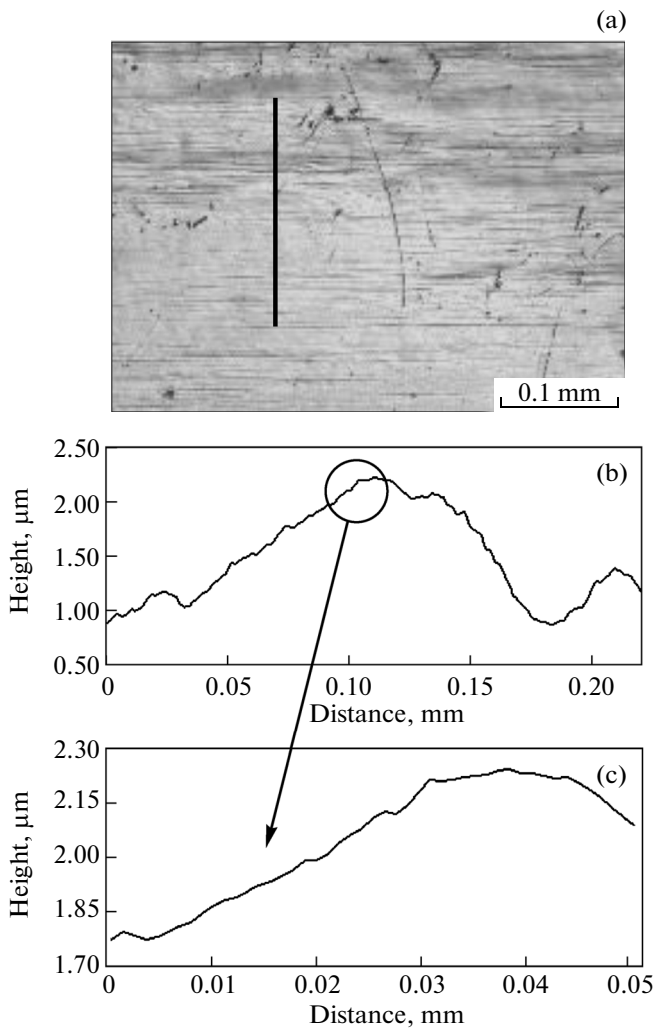
Fig. 2. (a) Deformation relief on the (112) lateral face of the nickel single crystal with [111] compression axis orientation after a 10% deformation with the indicated secants; (b, c) surface profiles along the corresponding secants.

it is interesting to note the fact that the Schmid factor increases to 0.35 in the regions with an orientation close to the [$\bar{1}$11] initial orientation with respect to the compression axis; for regions with the newly formed [110] orientation, the Schmid factor reaches 0.45. Hence, the material reorientation to the orientation for the most efficient slip can be observed.

An analysis of misorientation angles and their variation along the secant showed the results similar to those described above for folds formed normally to macroband systems: the misorientation angles within interlayers of the initial orientation are 2°–6°. The consideration of misorientation angle variations along the secant shows its periodic behavior. The maximum misorientation angles are observed with the same step of 5 μm as in the previous case. However, the misorientation angle at the boundaries of reoriented regions is appreciably larger and is ~30°–40°.

Let us discuss the causes of the observed folding features in the materials under study.

4. RESULTS AND DISCUSSION

The most intense folding is observed in studied materials in the maximum curvature region. One of such regions is the portion at the interface between beading and material bulk. The beading is caused by the stressed state scheme and the presence of end friction.

The bending and folding of the sample faces of the faces in the central region where the uniaxial compression scheme is implemented are caused by incompatible deformation of neighboring domains. In this case, folding at moderate degrees of deformation depends strongly on the orientation of single-crystal deformation axis and lateral faces.
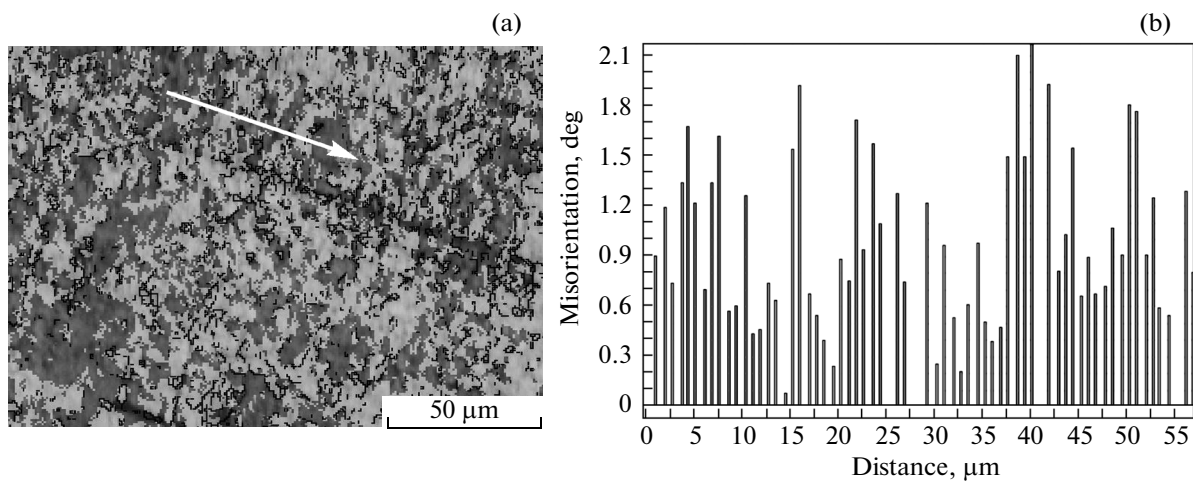

Fig. 3. Geometrical image of (a) boundaries and (b) misorientation along the secant (the secant direction is indicated by the arrow).

Simultaneously, the shearing method during slip along octahedral planes has an effect on folding. As shown in [5, 7], the slip can be accompanied by the formation of slip trace arrays, meso- and macrodeformation bands on the crystal surface, depending on the single-crystal orientation. The susceptibility to the formation of slip trace arrays depends on the SFE. Slip trace arrays are most intensely formed in alloys with low SFEs. The formation of the above relief structural elements on the crystal surface determines the periodic surface profile, which provides sample shape change under an external load. Our studies [7, 9] showed that the periodic surface profile efficiently promotes deformation inhomogeneity lowering. This is achieved by the following ways: (i) slip along parallel planes with periodic shear alternation, (ii) coordinated deformation in the bulk when forming meso- and macrodeformation bands, and (iii) folded structure formation on the surface.

The folding in the surface layer is probably associated with dislocation glide. Shearing at lower stresses is promoted by lower shear stability of the surface layer [10]. Both compression and tensile stresses take place in folding regions (mostly the regions of bending of the sample faces) [11]. They can activate or retard slip in local regions. Complex curvature promotes development of different folding types.

Accumulation of excess dislocation density and misorientations in local regions can be promoted by the retarded shear or the force moment effect on mesoregions. Most likely, the latter case is implemented at the interface of regions with different stressed state schemes [6, 12].

5. CONCLUSIONS

The analysis of the data obtained revealed that the prime cause of folding is the bending of the sample faces. Bending regions are preferred for folding. In this case, the degree of sample bending in a region affects the fold size, and the degree of curvature affects the fold morphology.

The folding is also significantly affected by the stressed state scheme and sample crystallography. In the near-end region, the fold (beading) is always formed. The orientation of shear directions with respect to the applied load and free surfaces is important when considering the shear crystallography. In this case, the less symmetric is the orientation of shear planes with respect to sample faces, the more pronounced is the folding process.

The data of the EBSD analysis demonstrated that the folding process is associated with the accumulation of the excess density of dislocations of the same sign and the formation of misoriented substructures in material surface layers. This is promoted by higher homologous deformation temperatures and stacking fault energies.

Furthermore, it was shown that the lattice rotation can be a deformation mechanism along with the octahedral slip.

REFERENCES

1. V. V. Gubernatorov, T. S. Sycheva, L. R. Vladimirov, V. S. Matveeva, A. I. Pyatygin, and M. B. Mel'nikov, Fiz. Mezomekh. **5** (6), 95 (2002).

2. V. V. Gubernatorov, L. R. Vladimirov, T. S. Sycheva, and D. V. Dolgikh, Fiz. Mezomekh. **4** (5), 97 (2001).

3. V. V. Gubernatorov, B. K. Sokolov, I. V. Gervas'eva, and L. R. Vladimirov, Fiz. Mezomekh. **2** (1−2), 157 (1999).

4. V. V. Gubernatorov, B. K. Sokolov, L. R. Vladimirov, A. K. Sbitnev, and I. V. Gervas'eva, Dokl. Akad. Nauk **364** (4), 468 (1999).

5. D. V. Lychagin, Fiz. Mezomekh. **9** (3), 103 (2006).

6. D. V. Lychagin, E. A. Alferova, and V. A. Starenchenko, Fiz. Mezomekh. **13** (3), 75 (2010).

7. E. A. Alferova, A. D. Lychagin, D. V. Lychagin, and V. A. Starenchenko, Fundam. Probl. Sovrem. Materialoved. **9** (2), 218 (2012).

8. O. A. Kaibyshev and R. Z. Valiev, *Grain Boundaries and Properties of Metals* (Metallurgiya, Moscow, 1987) [in Russian].

9. E. A. Alfyorova and D. V. Lychagin, Appl. Mech. Mater. **379**, 66 (2013).

10. V. E. Panin and A. V. Panin, Fiz. Mezomekh. **8** (5), 7 (2005).

11. S. I. Gubkin, *Plastic Deformation of Metals* (United States Joint Publications Research Service, Washington, 1960; Metallurgizdat, Moscow, 1961).

12. V. E. Panin and V. E. Egorushkin, Fiz. Mezomekh. **14** (3), 7 (2011).

Translated by A. Kazantsev